Environ Monit Assess (2011) 179:605–617
DOI 10.1007/s10661-010-1766-z

Assessment of spatial distribution of soil loss over the upper basin of Miyun reservoir in China based on RS and GIS techniques

Tao Chen · Rui-qing Niu · Yi Wang · Ping-xiang Li · Liang-pei Zhang · Bo Du

Received: 6 April 2010 / Accepted: 21 October 2010 / Published online: 9 November 2010

Abstract Soil conservation planning often requires estimates of the spatial distribution of soil erosion at a catchment or regional scale. This paper applied the Revised Universal Soil Loss Equation (RUSLE) to investigate the spatial distribution of annual soil loss over the upper basin of Miyun reservoir in China. Among the soil erosion factors, which are rainfall erosivity (R), soil erodibility (K), slope length (L), slope steepness (S), vegetation cover (C), and support practice factor (P), the vegetative cover or C factor, which represents the effects of vegetation canopy and ground covers in reducing soil loss, has been one of the most difficult to estimate over broad geographic areas. In this paper, the C factor was estimated based on back propagation neural network and the results were compared with the values measured in the field. The correlation coefficient (r) obtained was 0.929. Then the C factor and the other factors were used as the input to RUSLE model. By integrating the six factor maps in geographical information system (GIS) through pixel-based computing, the spatial distribution of soil loss over the upper basin of Miyun reservoir was obtained. The results showed that the annual average soil loss for the upper basin of Miyun reservoir was 9.86 t ha^{-1} ya^{-1} in 2005, and the area of 46.61 km^2 (0.3%) experiences extremely severe erosion risk, which needs suitable conservation measures to be adopted on a priority basis. The spatial distribution of erosion risk classes was 66.9% very low, 21.89% low, 6.18% moderate, 2.89% severe, and 1.84% very severe. Thus, by using RUSLE in a GIS environment, the spatial distribution of water erosion can be obtained and the regions which susceptible to water erosion and need immediate soil conservation planning and application over the upper watershed of Miyun reservoir in China can be identified.

Keywords Soil loss · RUSLE · BP neural network · GIS · Remote sensing · Miyun reservoir

T. Chen (✉) · R.-q. Niu · Y. Wang
Institute of Geophysics and Geomatics, China University of Geosciences, 430074, Wuhan, China
e-mail: tonychen21@gmail.com

P.-x. Li · L.-p. Zhang
State Key Lab of Information Engineering in Surveying, Mapping and Remote Sensing, Wuhan University, 430079, Wuhan, China

B. Du
Computer School, Wuhan University, 430079, Wuhan, China

Introduction

Soil erosion is a widespread problem in agriculture in the developing countries. The problem has far-reaching economic, political, social, and envi-

ronmental implications due to both on-site and off-site damages (Thampapillai and Anderson 1994; Grepperud 1995). The Miyun reservoir, which sits on Chaobaihe River, is the main surface source of the drinking water for Beijing, the capital of China, with the population of 14.93 million. Water and soil loss from agricultural, pastoral, and forestry lands is the main reason for sediment entering the reservoir, this process potentially has an impact on the safety of water supply for Beijing, and on the operation and life span of the reservoir (Zhou and Wu 2005). In terms of erosion, the soils are under a serious risk due to hilly topography, soil conditions facilitating water erosion (i.e., fine texture, low organic mater, and poor plant coverage due to semi-arid climate), and inappropriate agricultural practices such as excessive soil tillage and cultivation of steep lands. This widespread problem threatens the sustainability of agricultural productivity in Miyun reservoir watershed where economically important diverse crops are produced. In order to protect the water quality, it is necessary to reduce the soil erosion and improve the environment over the upper stream of Miyun reservoir (Yang et al. 2005). Since the reservoir operated, a series of environmental measures, which have obvious effect, such as water protection, afforestation, conversion of farmland back to forests or grassland, and so on (Gao 1999; Yu et al. 2004), have been taken to restore the deteriorated land. As there is still a lot of land that suffered or suffering from soil erosion, the evaluation of the current situation of erosion is very important for improvement of endangered areas, and determining the type of conservation measures to be applied; it is very crucial to estimate the status of soil erosion, especially for its spatial distribution, at regional-scale for sustainable management and conservation of the agricultural areas.

There are many researches of using soil erosion models such as the Universal Soil Loss Equation (USLE) (Wischmeier and Smith 1978) and its subsequent Revised Universal Soil Loss Equation (RUSLE) (Renard et al. 1997) and geographical information system (GIS) techniques to make soil erosion estimation and its spatial distribution (Wang et al. 2003a, b; López-Vicente and Navas 2009; Onori et al. 2006; Fu et al. 2005). In these two widely used models, the effect of vegetation is accounted for in the vegetation cover factor or *C* factor. In both models, the average soil erosion per year is computed from the product of six factors, namely: rainfall erosivity (*R*), soil erodibility (*K*), slope length (*L*), slope steepness (*S*), vegetation cover (*C*), and support practice factor (*P*). From the standpoint of soil conservation planning, the *C* factor is the most essential because the land-use changes that are meant to reduce soil erosion are represented by this factor.

The *C* factor has been one of the most difficult USLE or RUSLE factors to estimate over broad geographic areas. Traditionally, spatial estimates of vegetation cover, or *C* factor, have been done by simply assigning *C* factor values from literature or field data into a classified land cover map (cover classification method) (Folly et al. 1996; Juergens and Fander 1993; Morgan 1995). This method, however, resulted in *C* factor estimates that are constant for relatively large areas, and do not adequately reflect the spatial variation in vegetation that exists within large geographic areas (Wang et al. 2002). Errors in classification are also introduced in the *C* factor map. To increase the spatial variability and decrease the influence of classification errors, direct linear regression has been performed between image bands or ratios and *C* values determined in the field (Cihlar 1987; Stephens and Cihlar 1982). Gertner et al. (2002) and Wang et al. (2002, 2003a, b) used joint sequential co-simulation with Landsat TM images for mapping the *C* factor from point values. However, this method is costly and obtaining the appropriate number of sampling points for interpolation is rather difficult.

Vegetation indices such as Normalized Difference Vegetation Index (NDVI) have also been explored for mapping the *C* factor by relating it directly to USLE and RUSLE-*C* factor by regression analysis. However, satellite image-driven vegetation indices were found to have low correlation with the *C* factor (De Jong 1994; Tweddales et al. 2000). De Jong (1994) explained that the low correlation is due to the sensitivity of vegetation to vitality, as the condition of the vegetation is not always related to its soil protective function. Despite these issues, the NDVI is one of the commonly used methods to determine the *C* factor using remote sensing

for soil erosion assessment over regional or large geographic area (e.g., Cartagena 2004; De Jong et al. 1999; Hazarika and Honda 2001; Lin et al. 2002, 2006; Lu et al. 2003; Najmoddini 2003; Symeonakis and Drake 2004; Van der Knijff et al. 2002).

Other than the USLE and RUSLE, the *C* factor is also applied to other erosion models such as the Morgan and Finney method (Morgan et al. 1984), ANSWERS (Beasley et al. 1980), WEPP (NSERL 1995), SEMMED (De Jong and Riezebos 1997), and PCARES (Paningbatan 2001). Thus, it is important to improve the ways in which the *C* factor is estimated using remote sensing. A reliable vegetation cover factor estimate is essential for accurate identification and estimation of soil erosion, which in turn, is needed for sound conservation planning.

In this paper, back propagation (BP) neural network is used to map *C* factor values, and the results are compared with the values measured in the field. Then the *C* factor and the other factors were used as the input to RUSLE model in GIS through pixel-based computing to obtain the spatial distribution of soil loss over the upper watershed of Miyun reservoir. Therefore, the objective of this study was to use remote sensing data and GIS technique to estimate the spatial distribution of soil loss over the upper watershed of Miyun reservoir by using the RUSLE model. Then the regions which are susceptible to water erosion and need immediate soil conservation planning and application over the upper watershed of Miyun reservoir in China can be identified.

Materials and methods

Study area

The Miyun reservoir watershed is located in the north area of Beijing (Fig. 1), between 40°19′–41°38′ N and 115°25′–117°35′ E with an area of about 15,788 km^2. The northwest part of the study area is gently mountainous while the southeast part is mainly hilly and partially plain. The altitude varies between 150 and 1,800 m above sea level.

Climate conditions in the area reflect the typical continental monsoon climate with 488.9 mm annual average rainfall. Distribution of precipitation is generally decreasing from southeast to northwest, and precipitations are concentrated between July and September. Annual average temperatures in upper and lower watershed are 9°C and 25°C, respectively.

In the region the soil layer is thin. According to Chinese Soil Taxonomy (Chinese Soil Taxonomy Research Group 1995), mountain meadow soil, brown forest soil, and cinnamon soil are the main soil taxa. The annual average soil erosion measured at the reservoir (Chinese River Sediment Bulletin 2006) is 12–16 ton/ha and the annual amount of bedloads is about 5.72 million tons. The region suffers severe soil erosion and it is considered a priority area for soil conservation project in China in twenty-first century (Chinese River Sediment Bulletin 2006).

Satellite data image pre-processing

Four scenes of Landsat ETM+ images at spatial resolution of 30 m acquired on November 14, 2005, and November 21, 2005, were procured in this study. Besides geometric correction, an atmospheric correction is required to keep images consistent. The raw image data were processed by the ENVI 4.4 software.

A digital elevation model (DEM) with a spatial resolution of 30 m was derived from topographical map at 1:50,000 scale, surveyed by State Bureau of Surveying and Mapping in 1980s.

The land use/cover maps at 1:50,000 scale in the study area were used to valid the classes of the land cover (Institute of Geographic Sciences and Natural Resources Research, CAS in 1989s). The classes of land cover include farmland, forest land, grass land, water area, construction area, sandy land, meadow land, alkaline land, naked soil, and naked rock.

Field data collection

Fieldwork was conducted on several occasions in the upper watershed of Miyun reservoir during the same month the images were taken. The fieldwork basically involved the measurement of the *C* factor estimation. Normally, the *C* factor is evaluated from long-term experiments where

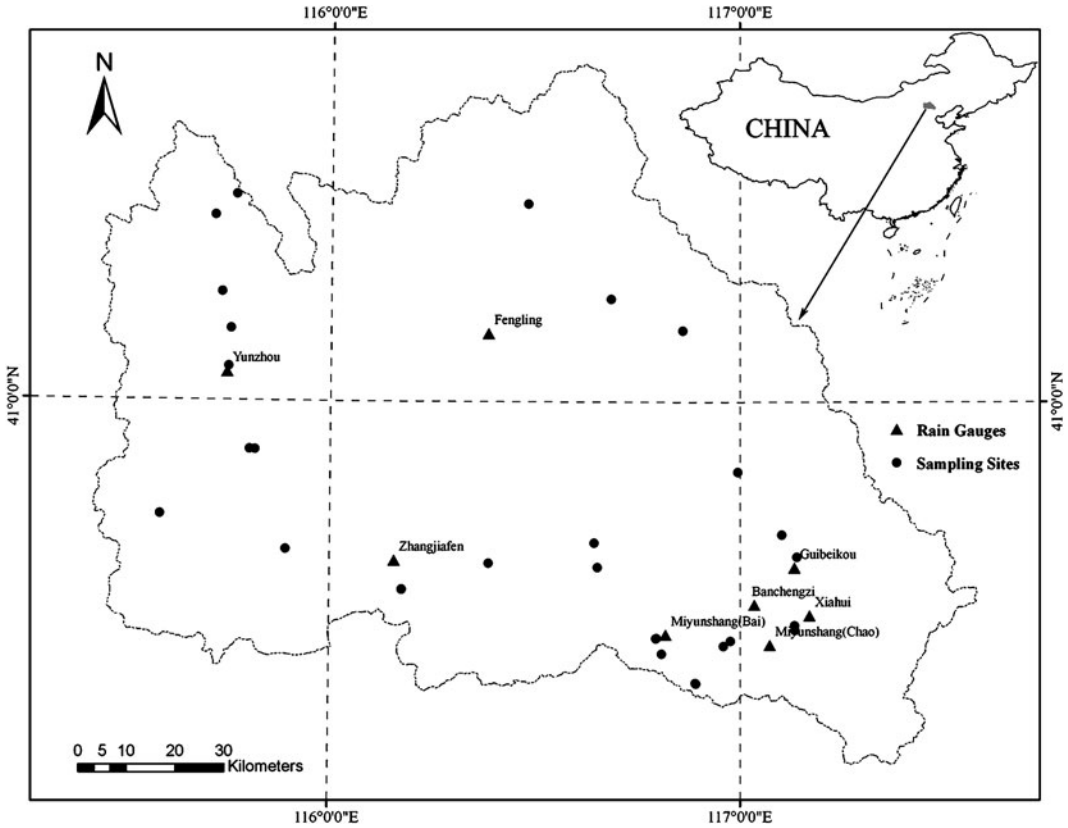

Fig. 1 Location of the rain gauges and sampling sites

soil loss is measured from field plots. However, in the absence of long-term experimental data, it is possible to estimate the *C* factor by using subfactors, which are percentage of ground cover and bare soil. Prior to the fieldwork, a detailed examination of False Color Composite of a Landsat ETM+ image and a topographic map of the study area was conducted to get an overall view and to systematically identify and select sampling areas for the *C* factor evaluation. A GPS was used to locate and define the sampling areas. Using the GPS, the Landsat ETM+ pixels that correspond to a 90 × 90-m area on the ground were identified (covering 9 pixels of Landsat ETM+). The distance error of the GPS is less than 5 m.

A total of 30 sampling sites were located and established in the study area (refer to Fig. 1). At each site, the percentage of vegetation cover and bare soil were estimated using the overhead photograph method. Measurements were taken by taking pictures at the sample plot with a vertical angle by using digital camera while the location of the sample plot were obtained by using GPS. An unsupervised classified method, maximum likelihood method, was used to classify the pictures into 10 classes. Then the 10 classes were classified into vegetation and bare soil again to compute the percentage of vegetation cover and bare soil. More than one picture was taken at one sample plot. Then the average value of the percentage of vegetation cover of them was taken as the measured *C* factor of the sample plot.

Methods

A model-based approach—RUSLE—was used to assess soil loss, because it is one of the least data demanding erosion models that has been developed and it has been applied widely at different scales. The RUSLE model was chosen because of its adaptability in estimating sheet and rill ero-

sion in tropical watersheds (Millward and Mersey 1999). The RUSLE is an updated version that retains the original structure of the USLE. Its main advantage is that, although developed to predict soil loss under temperate conditions, its use in other regions is possible by the determination of its factors from local data (Lu et al. 2003; Lufafa et al. 2003; Millward and Mersey 1999). Additional advantages include data requirements that are attainable under the limitations common in developing countries, and its compatibility with geographic information systems that allow for the prediction of erosion potential on a cell-by-cell basis (Millward and Mersey 1999).

In the RUSLE, the mean annual soil loss is expressed as a function of six erosion factors:

$$A = R \times K \times L \times S \times C \times P \quad (1)$$

where A is the computed amount of the average soil loss in tons per hectare per year, R the rainfall erosivity factor in megajoules per millimeter per hectare per hour per year, K the soil erodibility factor in tons per hour per megajoules per millimeter, L the slope length (meters), S the slope steepness (%), C the crop management factor, and P the erosion control practice factor. Factors C and P are dimensionless.

It has been very difficult to calculate the soil losses for the valley when a traditional sample method was used to collect the data for the RUSLE model. Based on field data, researchers in China have modified parameters and computing methods to suit reality. In this study, to develop the monitoring of soil losses in upper watershed of Miyun reservoir, remote sensing data, DEM, and land use and land cover GIS data were used. The values of parameters extracted from satellite sensor data and generated by GIS for the RUSLE model were pixel based (Table 1).

Table 1 Landsat ETM+ images used in the study

Image no.	Path/row	Date
1	123-031	Nov. 14, 2005
2	123-032	Nov. 14, 2005
3	124-031	Nov. 21, 2005
4	124-032	Nov. 21, 2005

Rainfall erosivity factor (R)

The rainfall erosivity index, R factor, in the USLE and RUSLE models, is an index of rainfall erosivity which is the potential ability of the rain to cause erosion. The energy of a given storm depends on all intensities at which the rainfall occurred and the amount of precipitation is associated with each intensity. However, among eight meteorological stations, there are only five that recorded the course of every storm. A storm's maximum 30-min precipitation intensity must be known to compute the storm's erosion index. If a station has not recorded 30-min intensities and only monthly and annual rainfall, the 30-min intensity of the nearest station was assumed to be representative. From long-term monthly and annual rainfall totals, and rainfall intensities from the five meteorological stations, the rainfall R factor for each station is found by Eq. 2 (Bu et al. 2003). Then R factor of the whole watershed was interpolated using a spline interpolation through GIS.

The computing formula is:

$$R_j = 0.1281 \times I_{30B} \times P_f - 0.1575 \times I_{30B} \quad (2)$$

where P_f is annual rainfall (mm), R is mean annual erosivity (MJ mm ha^{-1} h^{-1} ya^{-1}) and I_{30B} is a storm's maximum 30-min intensity (mm/h). The result for 2005 data in the form of an R erosivity map is shown in Fig. 2.

Soil erodibility factor (K)

The soil erodibility factor (K) represents both susceptibility of soil to erosion and the amount and rate of runoff, as measured under standard plot conditions. The soil data used in this study were collected and derived from the Second Soil Investigation in China. This investigation uses data on soil properties and maps of soil type distribution. Information on soil surface texture was derived. For each soil type, percentages of clay, silt, and sand were used to estimate K based on the class descriptions. K was estimated using Eq. 3 (Wischmeier and Smith 1978):

$$K = \left[2.1 \times 10^{-4} \times (12 - a) \times \left[Ss \times (100 - Sc)\right]^{1.14} + 3.25 \times (b - 2) + 2.5 \times (c - 3)\right] / 100 \times 0.1317 \quad (3)$$

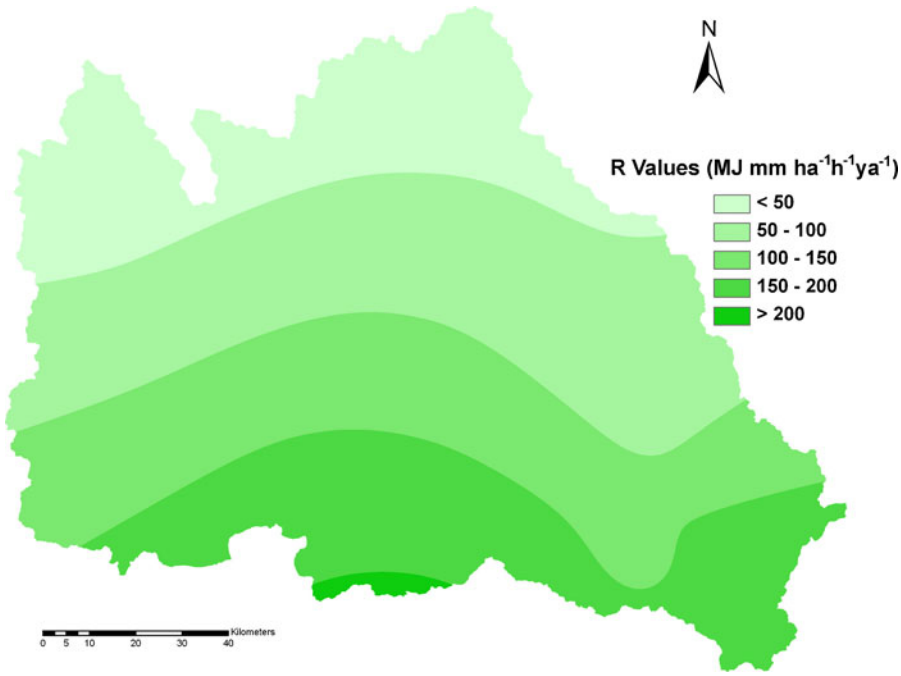

Fig. 2 *R* factor map of the study area

where K is the soil erodibility factor (t h MJ^{-1} mm^{-1}), Ss and Sc are the products of the dominant size component, and the percentage of the clay, respectively. α is the percentage of organic matter in %, b the soil structural (Table 2), and c the soil saturation capability (Table 3). Figure 3 shows spatially distributed of K values for different soil types in the watershed.

Cover factor (C)

In the USLE/RUSLE models, the cover factor (C) is an index which reflects, on the basis of the land use, the effect of cropping practices on the soil erosion rate. In this study, the factor C was calculated from the predominant crops using the back propagation neural network (Chen et al. 2008).

The BP algorithm is an error-based learning process consisting of two phases. The network can be activated by the input vectors in the first phase, and the output generated through the algorithm process. The error is defined as the difference between the network output and the desired output. The error is computed in the second phase, and is then propagated backward. The total square errors are fed from the output layer back through the hidden layers to the input layer, and the connection weights can be changed accordingly. This process is repeated until the error is below a certain value, which means the propagation reaches an acceptable precision. Then the network is properly trained, and is ready for prediction.

To achieve a proper training result, several parameters need to be set up, such as the network topology structure, the number of hidden layers, the number of nodes in each hidden layer, the learning rate, the initial weight value (evenly distributed in a small range to avoid the saturation of neurons) and the training iteration times (momentum factor to avoid partial minimization). Since the method is always ambiguous, many trials are needed before the best parameter values could be determined.

Many researchers built up the relationship between vegetation index and the vegetation cover,

Table 2 Soil structure status criteria

a (%)	≤0.5	0.51–1.5	1.51–4.0	≥4.0
B	4	3	2	1

Table 3 Soil saturation capability criteria

Sc (%)	≤10	10–15.9	16–21.6	21.7–27.4	27.5–39	>39.1
C	1	2	3	4	5	6

and obtained satisfied results (Dymond et al. 2005; Graetz et al. 1988; Purevdorj et al. 1998). In this paper, three vegetation indices and their different combination were taken as input layer to test the neural network, which were NDVI, soil adjust vegetation index (SAVI) and modified soil adjust vegetation index.

Finally, the network topology structure is shown in Fig. 4. The number of nodes in hidden layer is 6, and the NDVI and SAVI images are taken as the input values, and the *C* factors of Miyun reservoir watershed are the output layer. As a consequence of the Stone-Weierstrass theorem, all three-layer (one hidden layer) feed-forward neural networks whose neurons use arbitrary activation functions are capable of approaching any measurable function from one finite dimensional space to any desired degree of accuracy (Homik et al. 1989).

Conservation practices (*P*)

Because only a very small area has conservation practices, *P* factor values are assumed as 1 for the watershed.

Slope length and steepness factor (*LS*)

For *LS* calculations, the original USLE formula for estimating the slope length and slope steepness can be used (Wischmeier and Smith 1978). *LS* may be calculated from one of the three different functional forms of equation: linear, power, and polynomial. In this study, equation in power form is used. Liu et al. (2000) reported that an increase in the slope steepness from 20% to 40% and 60%, the slope length exponent did not change. Therefore, in the present study, separate equations for slope gradient <21% as given in the USLE Eq. 4

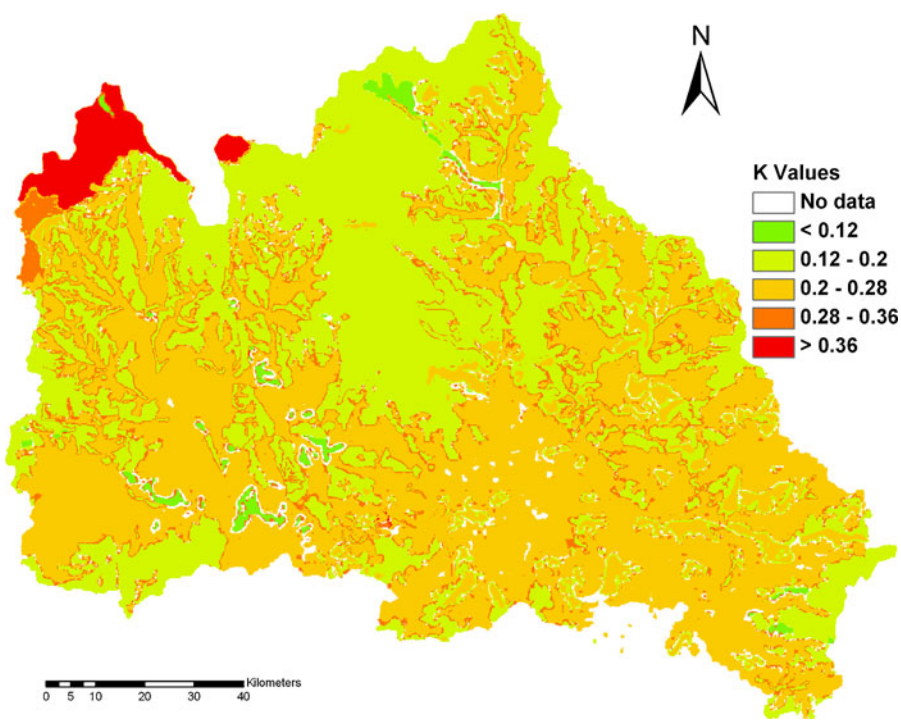

Fig. 3 *K* factor map of the study area

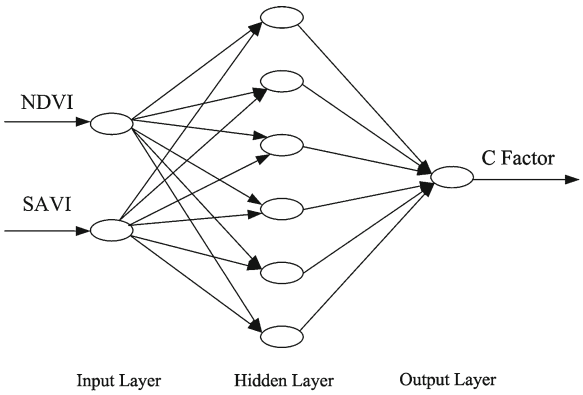

Fig. 4 Structure of the BP neural network used for *C* factor evaluation

and for areas with a slope gradient >21% as incorporated in the RUSLE, Eq. 5 have been used (Renard et al. 1997; Deore 2005).

$$LS = (L/22.1)^m \times (65.41 \times \sin^2\theta + 4.56 \times \sin\theta + 0.065) \quad (4)$$

$$LS = (L/22.1)^{0.7} \times \left[6.432 \times \sin\left(\theta^{0.79}\right) \times \cos\theta\right] \quad (5)$$

where L is slope length in meters; θ is angle of the slope; m is an exponent that depends on slope steepness (0.5 for slopes $\leq$ 5%, 0.4 for slopes $\leq$ 4%, and 0.3 for slopes $\leq$ 3%). m was taken 0.5 for slopes between 5% and 21% and 0.3 for slopes <5% in Eq. 4. Then the *LS* factor map is obtained and shown in Fig. 5.

Spatial distribution of soil loss

After completing data input procedure and preparation of *R*, *K*, *CP*, and *LS* maps as data layers, they were multiplied in the GIS to provide erosion risk map which shows spatial distribution of soil loss in the study area. Average soil loss was calculated as the product of each pixel value multiplied by pixel area.

In the China national professional standard of SL190-96 Standards for classification and Gradation of Soil Erosion (The Ministry of Water Resources of the People's Republic of China 1997), soil erosion intensity was divided into six grades as shown in Table 4. According to classification, erosion risk map based on distribution of soil loss over Miyun reservoir watershed was prepared.

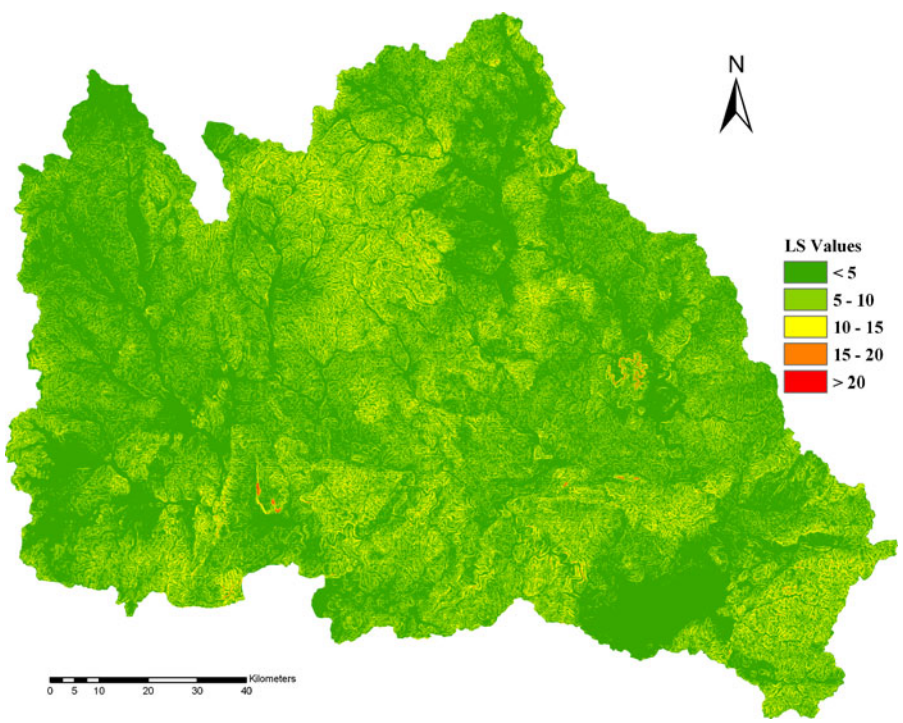

Fig. 5 *LS* factor map of the study area

Table 4 Soil erosion risk level and intensity

Erosion risk level	Intensity	Area (km^2)	Area (%)	Soil loss ($t\ ha^{-1}\ ya^{-1}$)
Lower	Slight	10,561.27	66.9	<10
Low	Light	3,455.23	21.89	10–25
Moderate	Moderate	974.99	6.18	25–50
High	Severe	456.1	2.89	50–80
Higher	Very severe	289.36	1.84	80–150
Highest	Extremely severe	45.73	0.3	>150

Results analysis and discussion

Results analysis

By using Eq. 2, *R* values of each station were calculated. Then the input maps of *R* factor of the whole watershed were interpolated using a spline interpolation through GIS (Fig. 2). This map shows the spatial distribution of *R* values of the upper watershed of Miyun reservoir. From Fig. 2, we can see that *R* values increased from northwest to southeast depending on precipitation characteristics. The minimum and maximum *R* value for the study area was 0.351 and 206.214 MJ mm $ha^{-1}\ h^{-1}\ ya^{-1}$ in 2005, respectively.

K values can be obtained by using Eq. 3. Different *K* values assigned for the mountain meadow soil, brown forest soil, and cinnamon soil groups for upper watershed and lower watershed. *K* values ranged from 0.117 to 0.3975 t h $MJ^{-1}\ mm^{-1}$ (Fig. 3).

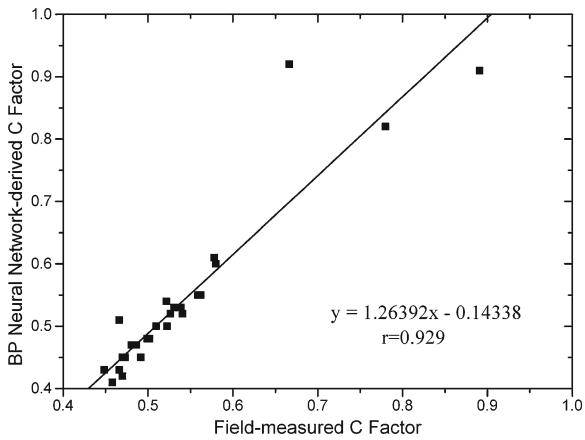

Fig. 6 Field-measured *C* factor versus BP neural network-derived *C* factor

C values were generated from the remote sensing data by using BP neural network method and field survey validation. Figure 6 shows the scatter plot correlations between the percentage of *C* values determined with the BP neural network and the field data from 30 sampling sites. The correlation coefficient (*r*) between the field measured vegetation cover and the one which is retrieved by the BP neural network is 0.929 with the standard deviation (SD) of 0.048. The *C* factor map derived using the BP neural network is shown in Fig. 7. The *C* factor values ranged from 0.0041 to 0.1089, which were higher in the low-lying place, because they can be affected by the man-made disturbance factor. *C* factor values of any place in the study area for USLE and RUSLE can be obtained from this map.

Because only a very small area has conservation practices, *P* factor values are assumed as 1 for the watershed.

In this paper, a topography map with a spatial resolution of 30 m was used to develop a map of the slope length and slope steepness factor (*LS*) by using Eqs. 4 and 5 which depending on slope smaller than 21% or more. The map obtained showed that *LS* values are directly related with the surface relief. *LS* values were higher in the mountains area than other place in Miyun reservoir (Fig. 5). The highest *LS* value for the reservoir was calculated as 20.63.

When *R*, *K*, *CP*, and *LS* factor maps were obtained, the soil loss map were generated by considering *R*, *K*, *CP*, and *LS* data layers (Fig. 8). Spatial distribution of soil loss with area is given in Table 4.

Annual average soil loss for the Miyun reservoir watershed was estimated as 9.86 t $ha^{-1}\ ya^{-1}$ in 2005. Almost half of the Miyun reservoir watershed (66.92%) falls into very low erosion risk class where soil loss is lower than 10 t $ha^{-1}\ ya^{-1}$.

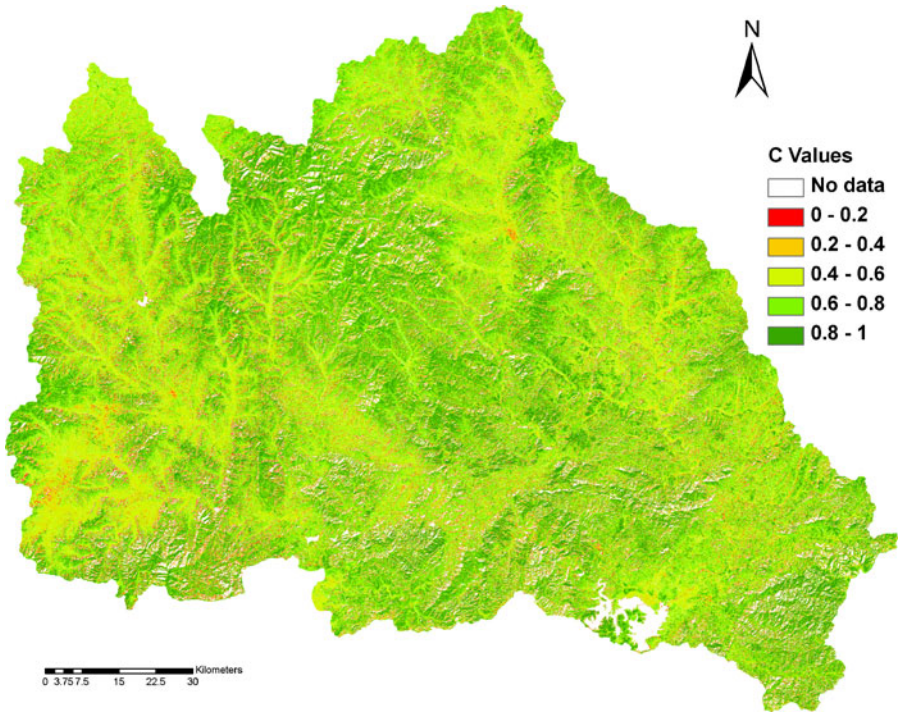

Fig. 7 *C* factor map of the study area derived using BP neural network method

Soil loss increases from east to west of the watershed. Sediment yield measurements in east (station name, Xiahui) and west (station name, Zhangjiafen) support our results (Table 5). Maximum soil loss was found more than 150 t ha^{-1} ya^{-1} at pixel level in the northwest part of watershed.

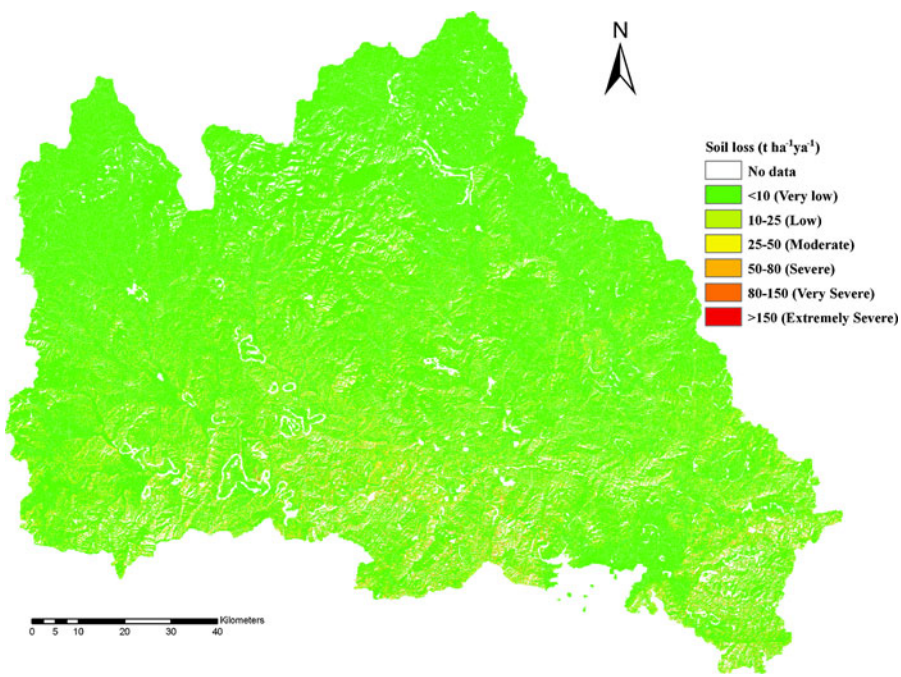

Fig. 8 Spatial distribution map of soil loss in the study area evaluated by the RUSLE method

Table 5 Measured sediment yields in the study area (Chinese River Sediment Bulletin 2006)

Station name	Location	Years of observations	Area (km^2)	Measured average sediment yield ($t\ ha^{-1}\ ya^{-1}$)	Amount of the sediment ($t\ ya^{-1}$)
XiaHui	117°9′29″ 40°37′37″	45	6,229.71	1.7	902,000
Zhangjiafen	116°47′49″ 40°35′13″	45	9,558.29	1.27	1,080,000

The high range of estimated of average amount of soil loss, more than acceptable soil loss tolerance (10 t ha^{-1} ya^{-1}) is found primarily in the lower area of the watershed. The study shows that 5.03% (793.83 km^2) area is under severe, very severe, and extremely severe erosion risk. This part of the watershed also has the highest average erosivity. Researchers using erosion simulation models indicated that erosion response is much more sensitive to rainfall amount and intensity than the other environmental variables (Nearing et al. 1990). In this area, priority must be given to protection of forest and afforestation of bare lands to reduce erosivity effects on soil loss.

An area about 0.3% (46.61 km^2) experiences extremely severe erosion risk, in this area soil loss was calculated more than 150 t ha^{-1} ya^{-1} at pixel level. This area needs suitable conservation measures to be adopted on a priority. Lower watershed is situated in flat plains, where the soil erosion by water is not active, but large percentage of these areas is located in regions with severe erosion potential, where the inappropriate cultivation practices or crop rotation result in accelerated soil erosion.

Results discussion

The results obtained are affected by some uncertainties which are associated with several factors. The simplified Eq. 2 proposed by Bu et al. (2003) was used in this paper to obtain *R* factor is the first uncertainty. The second uncertainty is associated with the *K* factor which was computed by means of a general relationship Eq. 3. The *C* factor which was generated by using BP network is the third uncertainty.

Furthermore, setting the *P* factors to 1 means that the Miyun reservoir catchment is an area without any specific support practice. Obviously, this is not real and implies that soil loss is overestimated. Thus, further analysis is necessary so that these factors are assigned more likely values.

Conclusion

The goal of this study was to assess the spatial distribution of soil loss over the Miyun Catchment (North China) for planning appropriate conservation measures. The model used to calculate average annual soil loss was the Revised Universal Soil Loss Equation. With a good correlation relationship of 0.929, the method offers a reliable estimate of the *C* factor on a pixel-by-pixel basis, which is useful for spatial modeling of soil erosion using the RUSLE model. Based on the BP neural network, the *C* factor values can be easily estimated by remote sensing data with its spatial distribution.

From the map of spatial distribution of soil loss, it showed that the average soil loss found 9.86 t ha^{-1} ya^{-1} in the watershed. More than half of the watershed area is under very low water erosion risk. Soils susceptible to erosion with a soil loss more than 10 t ha^{-1} ya^{-1} are found primarily in the lower watershed with regard to the spatial variation. The main reason for this is the close relationship with vegetation cover, rainfall–runoff erosivity, and also associated with the slopes. Sediment yield measurements verified the results. In this area, priority must be given for protection of forest and afforestation of steep bare lands and maximize plant coverage by rotation practices in the agricultural lands. Generated soil loss map is also able to indicate high erosion risk areas to soil conservationist and decision maker. But, because of the limitation of RUSLE, spatial

heterogeneity in the catchment, use of empirical data, and soil deposition in the catchment, there are uncertainties in the predicated value, in further studies, more attention should be on the possibilities for coupling RUSLE with models of routing sediments, such as the sediment delivery ratio to overcome this limitation.

Acknowledgements This work was supported by the National Natural Science Foundation of China under Grant No. 40901205, the open fund of Key Laboratory of Agrometeorological Safeguard and Applied Technique, CMA under Grant No. AMF200905, and the open fund of State Key Lab of Information Engineering in Surveying, Mapping & Remote Sensing, Wuhan University under Grant No. 09R02.

References

Beasley, D. B., Huggins, L. F., & Monke, E. J. (1980). ANSWERS: A model for watershed planning. *Transactions of the American Society of Agricultural Engineers, 23*(4), 938–944.

Bu, Z. H., Tang, W. L., Yang, L. Z., Xi, C. F., Liu, F. X., Wu, J. Y., et al. (2003). The progress of quantitative remote sensing method for annual soil losses and its application in Taihu-Lake catchments. *Acta Pedologica Sinica, 40*(1), 1–9. (in Chinese).

Cartagena, D. F. (2004). *Remotely sensed land cover parameter extraction for watershed erosion modeling*. MSc. Thesis, International Institute for Geo-information Science and Earth Observation, Enschede, The Netherlands, ITC publications.

Chen, T., Li, P. X., & Zhang, L. P. (2008). Retrieving vegetation cover by using BP neural network based on "Beijing-1" microsatellite data. In *The international conference on earth observation data processing and analysis (ICEODPA2008), 28–30 December 2008, China*.

Chinese River Sediment Bulletin (2006). *The ministry of water resources of the People's Republic of China*.

Chinese Soil Taxonomy Research Group, Institute of Soil Science, Academia Sinica and Cooperative Research Group on Chinese Soil Taxonomy (1995) *Chinese soil taxonomy (revised proposal)*. Beijing: China Agricultural Science and Technology Press.

Cihlar, J. (1987). A methodology for mapping and monitoring cropland soil erosion. *Canadian Journal of Soil Science, 67*(3), 433–444.

De Jong, S. M. (1994). Derivation of vegetative variables from a Landsat TM image for modelling soil erosion. *Earth Surface Processes and Landforms, 19*(2), 165–178.

De Jong, S. M., Paracchini, M. L., Bertolo, F., Folving, S., Megier, J., & De Roo, A. P. J. (1999). Regional assessment of soil erosion using the distributed model SEMMED and remotely sensed data. *Catena, 37*(3–4), 291–308.

De Jong, S. M., & Riezebos, H. T. (1997). SEMMED: A distributed approach to soil erosion modelling. In A. Spiteri (Ed.), *Remote sensing '96: Integrated applications for risk assessment and disaster prevention for the Mediterranean* (pp. 199–204). Rotterdam: Balkema.

Deore, S. J. (2005). *Prioritization of micro-watersheds of upper Bhama Basin on the basis of soil erosion risk using remote sensing and GIS technology*. Ph.D. Thesis, Department of Geography, University of Pune.

Dymond, J. R., Stephens, P. R., Newsome, P. F., et al. (2005). Percent vegetation cover of a degrading rangeland from SPOT. *International Journal of Remote Sensing, 13*(11), 1999–2007.

Folly, A., Bronsveld, M. C., & Clavaux, M. (1996). A knowledge-based approach for C-factor mapping in Spain using Landsat TM and GIS. *International Journal of Remote Sensing, 17*(12), 2401–2415.

Fu, B. J., Zhao, W. W., Chen, L. D., et al. (2005). Assessment of soil erosion at large watershed scale using RUSLE and GIS: A case study in the loess plateau of China. *Land Degradation and Development, 16*, 73–85.

Gao, J. R. (1999). Construction and countermeasures of water protection forest in Miyun reservoir watershed of Beijing City. *Bull Soil Water Conservation*, 19, 1–6.

Gertner, G., Wang, G., Fang, S., & Anderson, A. B. (2002). Mapping and uncertainty of predictions based on multiple primary variables from joint co-simulation with Landsat TM image and polynomial regression. *Remote Sensing of Environment, 83*(3), 498–510.

Graetz, R. D., Pech, R. R., & Davis, A. W. (1988). The assessment and monitoring of sparsely vegetated rangelands using calibrated Landsat data. *International Journal of Remote Sensing, 9*(7), 1201–1222.

Grepperud, S. (1995). Soil conservation and government policies in tropical area: Does aid worsen the incentives for arresting erosion. *Agricultural Economics, 12*, 120–140.

Hazarika, M. K., & Honda, K. (2001). Estimation of soil erosion using remote sensing and GIS: Its valuation and economic implications on agricultural production. In D. E. Stott, R. H. Mohtar, & G. C. Steinhardt (Eds.), *Sustaining the global farm* (pp. 1090–1093). Purdue University and USDA-ARS National Soil Erosion Research Laboratory.

Homik, K., Stinchcombe, M., & White, H. (1989). Multilayer feed forward networks are universal approximators. *Neural Networks, 2*, 359–366.

Juergens, C., & Fander, M. (1993). Soil erosion assessment by means of Landsat-TM and ancillary digital data in relation to water quality. *Soil Technology, 6*(3), 215–223.

Lin, C. Y., Lin, W. T., & Chou, W. C. (2002). Soil erosion prediction and sediment yield estimation: The Taiwan experience. *Soil and Tillage Research, 68*(2), 143–152.

Lin, W. T., Lin, C. Y., & Chou, W. C. (2006). Assessment of vegetation recovery and soil erosion at landslides caused by a catastrophic earthquake: A case study

in Central Taiwan. *Ecological Engineering, 28*(1), 79–89.

Liu, B. Y., Nearing, M. A., Shi, P. J., & Jia, Z. W. (2000). Slope length effects on soil loss for steep slopes. *Soil Science Society of America Journal, 64*, 1759–1763.

López-Vicente, M., & Navas, A. (2009). Predicting soil erosion with RUSLE in Mediterranean agricultural systems at catchment scale. *Soil Science, 174*(5), 272–282.

Lu, H., Prosser, I. P., Moran, C. J., Gallant, J. C., Priestly, G., & Stevenson, J. G. (2003). Predicting sheetwash and rill erosion over the Australian continent. *Australian Journal of Soil Research, 41*(6), 1037–1062.

Lufafa, A., Tenywa, M. M., Isabirye, M., Majaliwa, M. J. G., & Woomer, P. L. (2003). Prediction of soil erosion in a Lake Victoria basin catchment using a GIS-based universal soil loss model. *Agricultural Systems, 76*(3), 883–894.

Millward, A. A., & Mersey, J. E. (1999). Adapting the RUSLE to model soil erosion potential in a mountainous tropical watershed. *Catena, 38*(2), 109–129.

Morgan, R. P. C. (1995). *Soil erosion and conservation* (2nd ed.). Essex: Longman Group Limited.

Morgan, R. P. C., Morgan, D. D. V., & Finney, H. J. (1984). A predictive model for the assessment of soil erosion risk. *Journal of Agricultural Engineering Research, 30*(1), 245–253.

Najmoddini, N. (2003). *Assessment of erosion and sediment yield processes using remote sensing and GIS: A case study in rose chai sub-catchment of Orumieh Basin, W. Azarbaijan*. MSc. Thesis, International Institute for Geo-information Science and Earth Observation, Enschede, The Netherlands, ITC publications.

Nearing, M. A., Deer-Ascough, L., & Laflen, J. M. (1990). Sensitivity analysis of the WEPP hillslope profile erosion model. *Transactions ASAE, 33*(3), 839–849.

NSERL (1995). WEPP user summary. National Soil Erosion Research Laboratory, US Department of Agriculture. http://topsoil.nserl.purdue.edu/nserlweb/weppmain/docs/readme.htm. Accessed 30 March 2007.

Onori, F., Bonis, P. D., Grauso, S., et al. (2006). Soil erosion prediction at the basin scale using the revised universal soil loss equation (RUSLE) in a catchment of Sicily (southern Italy). *Environment Geology, 50*, 1129–1140.

Paningbatan, E. P. (2001). Geographic information system-assisted dynamic modeling of soil erosion and hydrologic processes at a watershed scale. *Philippine Agricultural Scientist, 84*(4), 388–393.

Purevdorj, T. S., Tateishi, R., Ishiyama, T., et al. (1998). Relationships between percent vegetation cover and vegetation indices. *International Journal of Remote Sensing, 19*(18), 3519–3535.

Renard, K. G., Foster, G. A., Weesies, G. A., & McCool, D. K. (1997). *Predicting soil erosion by water: A guide to conservation planning with RUSLE*. USDA. Agriculture Handbook No. 703. Washington, DC.

Stephens, P. R., & Cihlar, J. (1982). Mapping erosion in New Zealand and Canada. In C. J. Johannsen, & J. L. Sanders (Eds.), *Remote sensing and resource management* (pp. 232–242). Ankeny: Soil Conservation Society of America.

Symeonakis, E., & Drake, N. (2004). Monitoring desertification and land degradation over sub-Saharan Africa. *International Journal of Remote Sensing, 25*(3), 573–592.

Thampapillai, D. A., & Anderson, J. R. (1994). A review of the socio-economic analysis of soil degradation problem for developed and developing countries. *Review of Marketing and Agricultural Econmics, 62*, 291–315.

The Ministry of Water Resources of the People's Republic of China (1997). National professional standards for classification and gradation of soil erosion, SL 190-1996.

Tweddales, S. C., Eschlaeger, C. R., & Seybold, W. F. (2000). *An improved method for spatial extrapolation of vegetative cover estimates (USLE/RUSLE C factor) using LCTA and remotely sensed imagery*. USAEC report No. SFIM-AEC-EQ-TR-200011, ERDC/CERL TR-00-7, US Army of Engineer Research and Development Center, CERL, Champaign, Illinois.

Van der Knijff, J., Jone, R. J. A., & Montanarella, L. (2002). *Soil erosion risk assessment in Italy*. European Soil Bureau, Joint Research Center of European Commission. EUR 19022EN.

Wang, G., Gertner, G., Fang, S., Anderson, A. B. (2003a). Mapping multiple variables for predicting soil loss by geostatistical methods with TM images and a slope map. *Photogrammetric Engineering and Remote Sensing, 69*(8), 889–898.

Wang, G., Gertner, G., Fang, S., et al. (2003b). Mapping multiple variables for predicting soil loss by geostatistical methods with TM images and a slope map. *Photogrammetric Engineering and Remote Sensing, 69*, 889–898.

Wang, G., Wente, S., Gertner, G. Z., & Anderson, A. (2002). Improvement in mapping vegetation cover factor for the universal soil loss equation by geostatistical methods with landsat thematic mapper images. *International Journal of Remote Sensing, 23*(18), 3649–3667.

Wischmeier, W. H., & Smith, D. D. (1978). *Predicting rainfall erosion losses: A guide to conservation planning, USDA*. Washington, DC: Agriculture Handbook No. 537.

Yang, D. Z., Xu, X. D., Liu, X. D., et al. (2005). Complex sources of air-soil-water pollution processes in the Miyun reservoir region. *Science in China Series D Earth Sciences, 48*(Supp. II), 230–245.

Yu, X. X., Niu, J. Z., & Xu, J. L. (2004). Effects of closing mountain for forest restoration in the watershed of Miyun reservoir Beijing. *Forestry Studies in China, 6*(3), 28–35.

Zhou, W. F., & Wu, B. F. (2005). Soil erosion estimation of the upriver areas of Miyun Reservoir located on the Chaobai River using remote sensing and GIS. *Transactions of the CSAE, 21*(10), 46–50.